Transaction B: Mechanical Engineering
Vol. 16, No. 3, pp. 197–211

SCIENTIA IRANICA

A Numerical Study of Flow and Heat Transfer Between Two Concentric Rotating Spheres with Time-Dependent Angular Velocities

A. Jabbari Moghadam[1] and A. Baradaran Rahimi[1,*]

Abstract. *The transient motion and heat transfer of a viscous incompressible fluid contained between two concentric spheres, maintained at different temperatures and rotating about a common axis with different angular velocities, is considered numerically, when the angular velocities are arbitrary functions of time. The resulting flow pattern, temperature distribution and heat transfer characteristics are presented for the various cases, including exponential and sinusoidal angular velocities. An interesting effect, of long delays in the heat transfer of a large portion of the fluid in the annulus, is observed, because of the angular velocities of the corresponding spheres.*

Keywords: *Flow and heat transfer; Concentric rotating spheres; Time-dependent angular velocities; Numerical solution.*

INTRODUCTION

The transient motion of an incompressible viscous fluid and its heat transfer in rotating spherical annuli is considered numerically, when the spheres are concentric and their angular velocities about a common axis of rotation are arbitrarily-prescribed functions of time. Such motions may be described in terms of a pair of coupled non-linear partial differential equations in three independent variables. It should be noted that the energy equation is linear when the velocity field is known.

Available theoretical works concerning such problems are primarily of a boundary-layer or singular-perturbation character considered by Howarth [1], Proudman [2], Lord & Bowden [3], Fox [4], Greenspan [5], Carrier [6] and Stewartson [7]. The first numerical study of a time-dependent viscous flow between two rotating spheres was presented by Pearson [8] in which the cases of one (or both) spheres is given an impulsive change in angular velocity, starting from a state of either rest or uniform rotation. Munson and Joseph [9] have considered the case of the steady motion of a viscous fluid between concentric rotating spheres, using perturbation techniques for small values of Reynolds number and a Legendre polynomial expansion for larger values of Reynolds number. Thermal convection in rotating spherical annuli has been considered by Douglass, Munson and Shaughnessy [10] in which the steady forced convection of a viscous fluid contained between two concentric spheres that are maintained at different temperatures and rotate about a common axis with different angular velocities is studied. Approximate solutions to the governing equations are obtained in terms of a regular perturbation solution valid for small Reynolds number and a modified Galerkin solution for moderate Reynolds numbers. Viscous dissipation is neglected in their study and all fluid properties are assumed constant. A study of viscous flow in oscillatory spherical annuli has been done by Munson and Douglass [11] in which a perturbation solution, valid for slow oscillation rates, is presented and compared with experimental results. Another interesting work is the study of the axially symmetric motion of an incompressible viscous fluid between two concentric rotating spheres done by Gagliardi et al. [12]. This work involves the study of the steady state and transient motion of a system consisting of an incompressible Newtonian fluid in an annulus between two concentric, rotating rigid spheres. The primary purpose of their research is to study the use of an approximate analytical method for analyzing the transient motion of the fluid in the annulus and

1. *Faculty of Engineering, Ferdowsi University of Mashhad, Mashhad, P.O. Box 91775-1111, Iran.*
*. *Corresponding author. E-mail: rahimiab@yahoo.com*

Received 16 January 2007; received in revised form 19 February 2008; accepted 10 March 2008

spheres which are started suddenly due to the action of prescribed torques. Their work is similar to the study by Jen-Kang Yang et al. [13] and the finite element study by Ni and Nigro [14]. The problems include the case where one or both spheres rotate with prescribed constant angular velocities and the case in which one sphere rotates due to the action of an applied constant or impulsive torque. Also, Bar-Yoseph et al. [15] consider the problem of the mixed-convection of rotating fluids in spherical annuli in which they focus on the formation of various secondary flow patterns in the meridional plane using the Galerkin finite element method. The thermal effects on an axisymmetric vortex breakdown in a spherical gap have also been considered by Arkadyev et al. [16] in which the influence of a temperature field on the vortex breakdown phenomenon is examined using a finite element formulation. The physical system considered is the spherical annulus between two concentric spheres with radii ratio 1:2, which is filled with a Boussinesq fluid; the outer sphere being stationary and hot while the inner sphere rotates and is at a lower temperature. The other work to mention is the study of an axisymmetric vortex breakdown for a generalized Newtonian fluid contained between rotating spheres by Bar-Yoseph and Kryzhanovski [17], with the purpose of providing a more complete understanding of the secondary flow structure of dilute suspensions in rotating systems. The physical system considered is the spherical annulus between two concentric spheres; radii 1:2, which is filled with a Boussinesq generalized Newtonian fluid and the walls of the spherical annulus being held at uniform but different temperatures. A weak penalty finite element formulation is also used in this problem. Besides, there are many studies considering natural convection. These include: Laminar natural convection about an isothermally heated sphere at small Grashof numbers by Fendell [18]; natural convection between two concentric spheres-transition towards a multicellular flow by Caltagirone et al. [19]; natural convection between concentric spheres at low Rayleigh numbers by Mack et al. [20]; natural convection between concentric spheres by Garg [21]; transient natural convection heat transfer between concentric spheres by Chu et al. [22]; transient natural convection heat transfer between concentric and vertically eccentric spheres by Chiu et al. [23]; and transient natural convection heat transfer of fluids with variable viscosity between concentric and vertically eccentric spheres by Wu et al. [24].

The study of the transient motion and heat transfer of an incompressible viscous fluid filling the annuli of two concentric spheres rotating with any prescribed function of time angular velocity has not been considered in the literature. In the present study, a numerical solution of unsteady momentum and energy equations is presented for viscous flow between two concentric rotating spheres maintained at different temperatures, which are rotating with time-dependent angular velocities. The results for some example functions including exponential and sinusoidal angular velocities are presented when the outer sphere initially starts rotating with a constant angular velocity and the inner sphere starts rotating with a prescribed time-dependent function. Similar physical and geometrical configurations are used in engineering systems and in designs like centrifuges and fluid gyroscopes, and also are important in geophysics and nuclear reactor designs, thermal energy storage cells and solar energy collectors. Other applications of the configuration used in this problem are in meteorological instrumentations where such apparatus and equipment are used to obtain quantitative information about the weather. An accurate prediction of steady state heat transfer rates and temperature distribution is required in these engineering design problems. For some engineering applications such as gyroscopes, the prediction of the transient temperature distribution and heat transfer rate from initial state to steady state is very important [8-11]. Sinusoidal rotation of the spherical containers are seen in all the mixers used in different types of industry and their stopping and starting movements are usually accomplished in an exponential manner.

PROBLEM FORMULATION

The geometry of the spherical annulus considered is indicated in Figure 1. A Newtonian, viscous, incompressible fluid fills the gap between the inner and outer spheres, which are of radii R_i and R_0, with constant surface temperatures, T_i and T_0, rotating about a common axis with angular velocities, Ω_i and Ω_0, respectively. The components of the velocity in directions

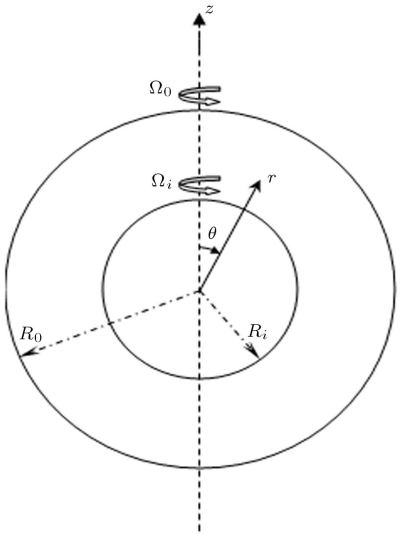

Figure 1. Spherical annulus.

r, θ and ϕ are v_r, v_θ and v_ϕ, respectively. These velocity components for incompressible flow and in a meridian plane satisfy the continuity equation, being related to stream function ψ and angular momentum function, Ω, in the following manner:

$$v_r = \frac{\psi_\theta}{r^2 \sin\theta}, \qquad v_\theta = \frac{-\psi_r}{r \sin\theta}, \qquad v_\phi = \frac{\Omega}{r \sin\theta}. \quad (1)$$

Since the flow is assumed to be independent of the longitude, ϕ, the non-dimensional Navier-Stokes equations and energy equation can be written in terms of the stream function and the angular velocity function as follows:

$$\frac{\partial \Omega}{\partial \tau} + \frac{\psi_\theta \Omega_r - \psi_r \Omega_\theta}{r^2 \sin\theta} = \frac{1}{(\mathrm{Re})} D^2 \Omega, \quad (2)$$

$$\begin{aligned} &\frac{\partial}{\partial \tau}(D^2\psi) + \frac{2\Omega}{r^3 \sin^2\theta}[\Omega_r r \cos\theta - \Omega_\theta \sin\theta] \\ &\quad - \frac{1}{r^2 \sin\theta}[\psi_r (D^2\psi)_\theta - \psi_\theta (D^2\psi)_r] \\ &\quad + \frac{2D^2\psi}{r^3 \sin^2\theta}[\psi_r r \cos\theta - \psi_\theta \sin\theta] \\ &\quad = \frac{1}{(\mathrm{Re})} D^4 \psi, \end{aligned} \quad (3)$$

$$\begin{aligned} &\frac{\partial T}{\partial \tau} + v_r \frac{\partial T}{\partial r} + \frac{v_\theta}{r}\frac{\partial T}{\partial \theta} \\ &\quad = \frac{1}{(\mathrm{Pe})}\left[\frac{\partial^2 T}{\partial r^2} + \frac{2}{r}\frac{\partial T}{\partial r} + \frac{1}{r^2}\frac{\partial^2 T}{\partial \theta^2} + \frac{\cot\theta}{r^2}\frac{\partial T}{\partial \theta}\right] \\ &\quad + (\mathrm{Ek})\left\{2\left[\left(\frac{\partial v_r}{\partial r}\right)^2 + \left(\frac{1}{r}\frac{\partial v_\theta}{\partial \theta} + \frac{v_r}{r}\right)^2 \right.\right. \\ &\quad \left. + \left(\frac{v_r}{r} + \frac{v_\theta}{r}\cot\theta\right)^2\right] + \left[r\frac{\partial}{\partial r}\left(\frac{v_\theta}{r}\right) + \frac{1}{r}\frac{\partial v_r}{\partial \theta}\right]^2 \\ &\quad \left. + \left[\frac{\sin\theta}{r}\frac{\partial}{\partial \theta}\left(\frac{v_\phi}{\sin\theta}\right)\right]^2 + \left[r\frac{\partial}{\partial r}\left(\frac{v_\phi}{r}\right)\right]^2\right\}, \end{aligned} \quad (4)$$

in which the non-dimensional Reynolds number (Re), Prandtl number (Pr), Peclet number (Pe) and Eckert number (Ek) are defined as:

$$\mathrm{Re} = \frac{\omega_0 r_0^2}{\nu}, \qquad \mathrm{Pr} = \nu/\alpha, \qquad \mathrm{Pe} = \mathrm{Re.\,Pr} = \frac{\omega_0 r_0^2}{\alpha},$$

$$\mathrm{Ek} = \frac{\nu \omega_0}{c_P (T_0 - T_i)}. \quad (5)$$

The following non-dimensional parameters have been used in the above equations, and then the asterisks have been omitted:

$$\tau^* = \tau\omega_0, \qquad r^* = \frac{r}{r_0}, \qquad \psi^* = \frac{\psi}{r_0^3 \omega_0},$$

$$\Omega^* = \frac{\Omega}{r_0^2 \omega_0}, \qquad T^* = \frac{T - T_i}{T_0 - T_i}, \quad (6)$$

in which r_0 and ω_0 are reference values. The non-dimensional boundary and initial conditions for the above governing equations are:

For $\tau \prec 0$:

$$\begin{cases} \psi = 0 \\ \Omega = 0 \\ T = 0 \end{cases}, \qquad \text{everywhere.}$$

For $\tau \geq 0$:

$$\theta = 0 \rightarrow \{\psi = 0,\ D^2\psi = 0,\ \Omega = 0\}, \qquad \frac{\partial T}{\partial \theta} = 0,$$

$$\theta = \pi \rightarrow \{\psi = 0,\ D^2\psi = 0,\ \Omega = 0\}, \qquad \frac{\partial T}{\partial \theta} = 0,$$

$$r = R_i/r_0 \rightarrow \begin{cases} \psi = 0,\ \psi_r = 0,\ \Omega = \frac{\Omega_i R_i^2}{\omega_0 r_0^2}\sin^2\theta \\ T = 0 \end{cases}$$

$$r = R_0/r_0 \rightarrow \begin{cases} \psi = 0,\ \psi_r = 0,\ \Omega = \frac{\Omega_0 R_0^2}{\omega_0 r_0^2}\sin^2\theta \\ T = 1 \end{cases} \quad (7)$$

where:

$$D^2 \equiv \frac{\partial^2}{\partial r^2} + \frac{1}{r^2}\frac{\partial^2}{\partial \theta^2} - \frac{\cot\theta}{r^2}\frac{\partial}{\partial \theta}. \quad (8)$$

These governing equations, along with the related boundary and initial conditions, are solved numerically in the next section.

COMPUTATIONAL PROCEDURE

The two equations governing the fluid motion show that each is describing the behavior of one of the dependent variables, Ω and ψ. On the other hand, these two equations are coupled only through nonlinear terms. To solve the problem numerically, the momentum equations were discretized by the finite-difference method using implicit-explicit schemes, which is a stabilizing technique. The number of iterations for the case of Re = 1000, for example, and a time-step of 0.01, are about 23000, which on a Pentium 4 computer takes around 48 hours to solve momentum and energy equations. Because of the known velocity field from momentum equations, the energy equation is linear and is solved here without neglecting any terms. In

each time step $(n+1)$, the value of the dependent variables are estimated from their values at previous time steps (n), $(n-1)$ and $(n-2)$ and, after using them in difference equations and repeating this, until the desired convergence is obtained. This will lead to the corrected values at this time step. This procedure is applied for the next time step.

The flow field considered is covered with a regular mesh (see Figure 2). To solve the system of linear difference equations, a tri-diagonal method is used in both directions, r and θ [25]. The direct substitution of previous values of dependent variables by new calculated values can provoke instability in numerical calculations in general. To overcome this problem, a weighting procedure is used in which the optimum weighting factor depends on the Reynolds number of the flow. The bigger the Reynolds number, the smaller the value of each quantity that is added to its previous value at each iteration (bigger weighting factor). Convergence is assumed when the ratio of every one of the quantities for the last two approximations differed from unity by less than 10^{-5} at all values of independent variable. A mesh independence study has been demonstrated in Figures 3 and 4. In this mesh-study, the conditions of flow and heat transfer fields are: Re $= 10$, Pr $= 10$, Ek $= 0$ and $\Omega_{io} = 0$. As can be seen, the difference between the contours of the ψ function for the coarse grid (case (a) with mesh size $25*12$) and the fine grid (case (b) with mesh size $40*20$) is almost large (about 12%), but the difference between case (c) (with grid size $45*25$) and case (d) (with grid size $50*25$) is really negligible (less than 0.03%). Hence, the numerical solution is mesh-independent for cases (c) or (d) and even (b). For the results presented in our solution, a $50*25$ mesh grid has been selected, although a $40*20$ mesh would have been fine. The mesh sizes mentioned above are in $\theta \times r$ directions. The contours of temperature have also been drawn for mesh sizes from case (a), $25*12$, to case (d), $50*25$, in Figure 4. Here, no significant differences between these cases can be seen and that is because the energy equation is linear and its solution has much fewer complexities compared with the momentum equation.

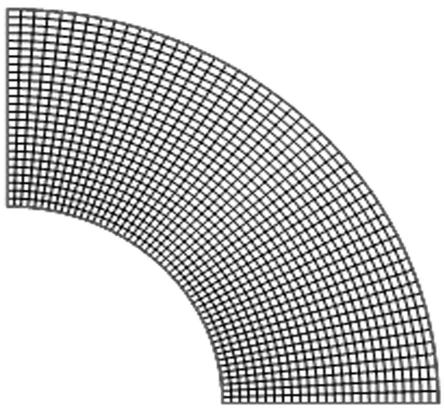

Figure 2. Mesh size.

The final results obtained in each case are exactly the results of the work of Pearson [8] and Munson and Joseph [9] for the Navier-Stokes equations and energy equation. To verify the validity of the numerical procedure used in this work, the numerical results of research studies such as [8-10] (see Figure 3), have been reproduced with the same flow parameters. These results, which are very close to our results obtained in these references, are shown in Figure 5.

In our study, these results have been obtained with a lot fewer computational complexities since they have been reached by solving an ordinary differential system of equations.

In this work, the sphere angular velocity has been considered as a function of time and in order to apply this time-function to the program, at the beginning of each time step the average of that time step has been calculated and used for the sphere angular velocity function. Therefore, for each considered time step, the sphere velocity is defined and assumed continuous at each cross section.

PRESENTATION OF RESULTS

If the bounding spherical surfaces were stationary, there would be no fluid motion and the temperature distribution would simply be due to conduction. Any rotation of the bounding spheres sets up a primary flow (ω) around the axis of rotation. This relative motion induces an unbalanced centrifugal force field, which drives the secondary flows (ψ) in the meridian plane. Thus, if the bounding spheres are of unequal temperature, this secondary flow produces forced convection within the annulus, resulting in a temperature distribution which is different from the pure conduction distribution. The relative magnitudes of the secondary flow and forced convection effects depend upon the parameters involved, including those concerning the geometry of the flow and those concerning the dynamics of the flow such as $\Omega_{io} = \Omega_i/\Omega_0$, $R_{io} = R_i/R_0$, Prandtl number and Reynolds number. These secondary flows known as vortex have a clockwise or counterclockwise motion, depending on whether the outer sphere or the inner sphere is dominant, as far as the secondary flow is concerned. To have a better understanding of the effect of secondary flows on temperature distribution, the contours of $(T - T_c)$ are also presented in this study, which show the difference between actual temperature and a pure conduction case. Here, T_c depends only on r. The cases considered here include time-dependent angular velocities, which are exponential and sinusoidal. The results for velocity and temperature fields are presented for cases when

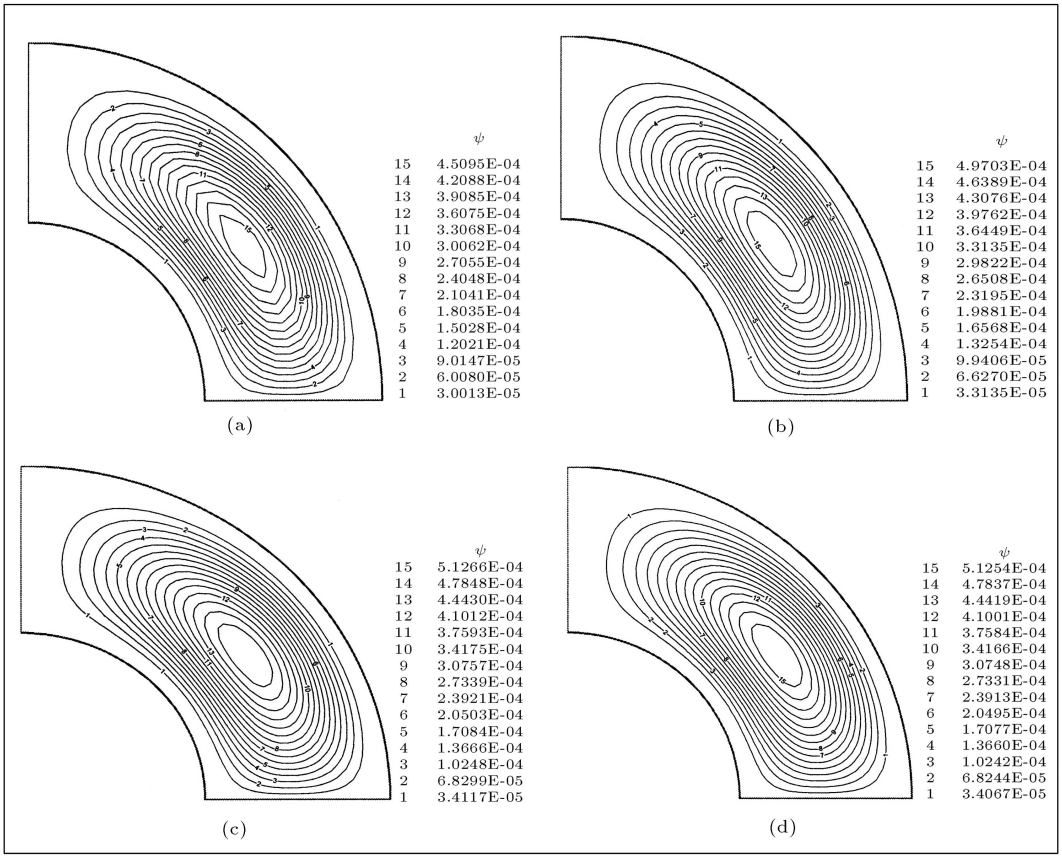

Figure 3. Contours of stream function for various mesh-size grid.

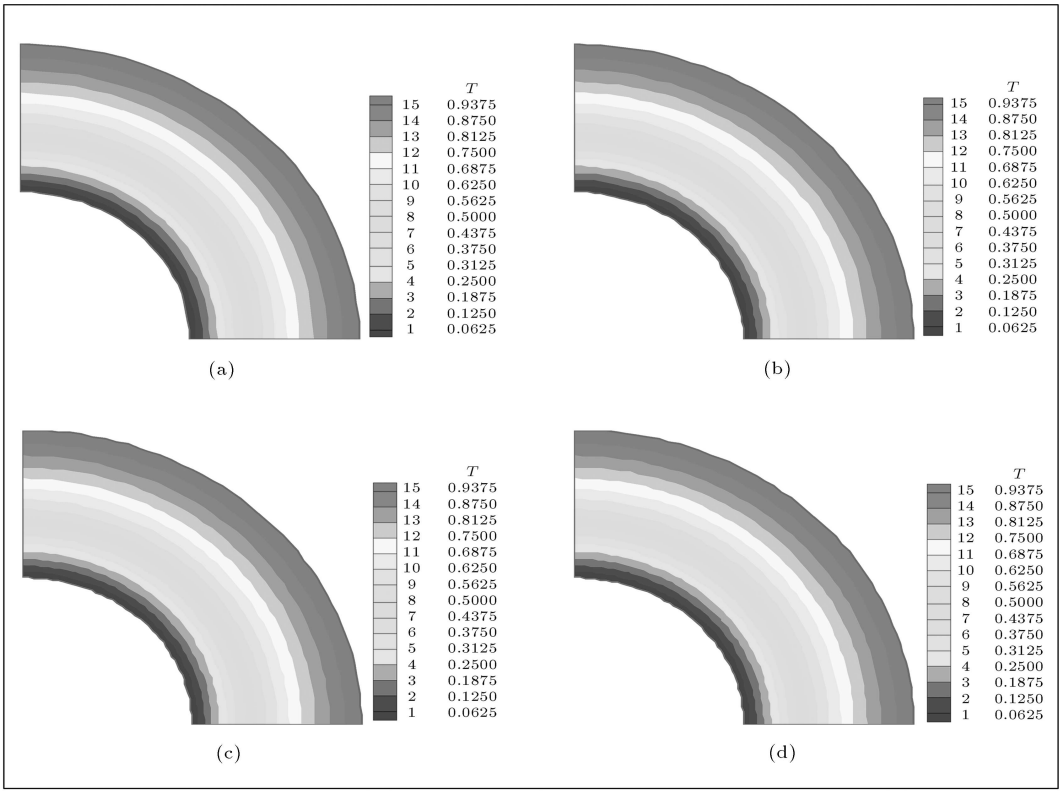

Figure 4. Contours of temperature for various mesh-size grid.

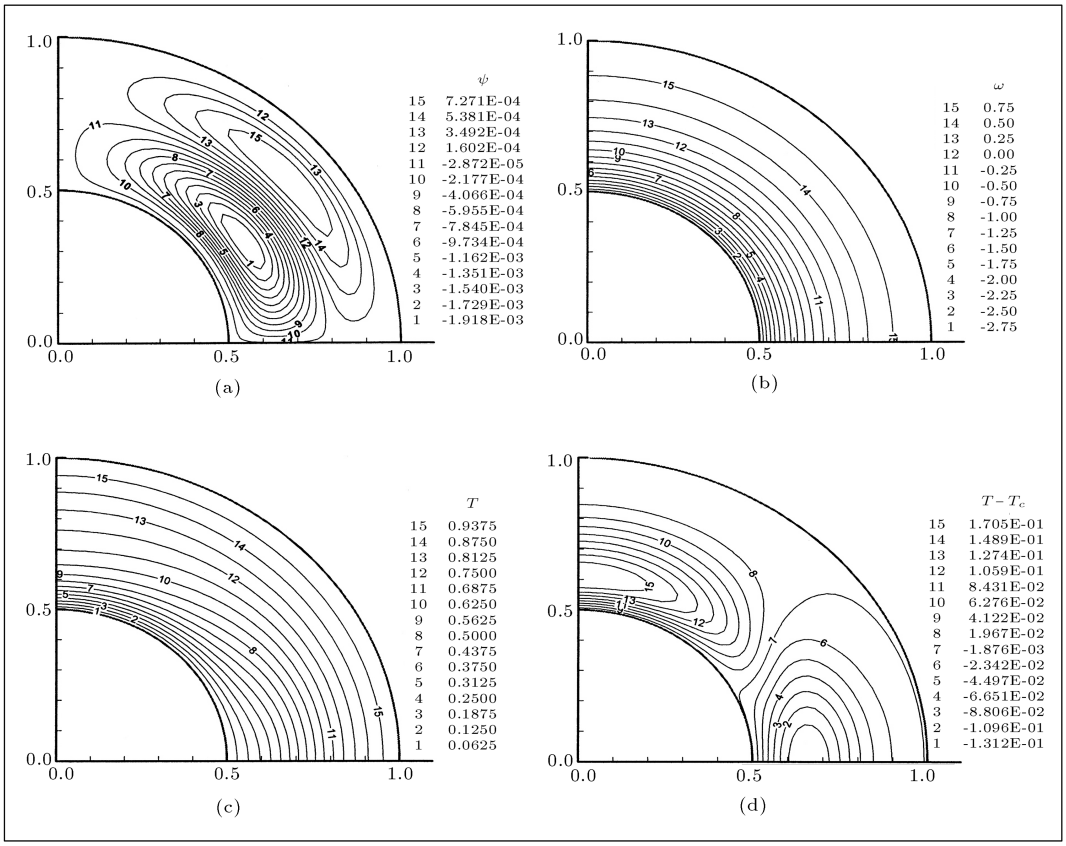

Figure 5. Velocity (or stream function) and temperature distribution for Re = 50, Pr = 10, Ek = 0 and $\Omega_{io} = -3$ at $t = 55.01$.

the outer sphere is rotating with a constant angular velocity and the inner sphere starts rotating with the prescribed function of time angular velocities. These presentations are only at some selected time values.

The velocity fields for the particular case of an inner sphere angular velocity $\Omega_{io} = -\exp(1-\tau)$ and an outer sphere rotating with constant angular velocity are presented in Figures 6 and 7 for Reynolds number Re = 1000 and at selected time values. At the beginning, when the vortices (ψ contours) are formed, it is observed that the annulus space is under the effect of both spheres that are dominating the flow field. A clockwise vortex close to the outer sphere and a counterclockwise vortex close to the inner sphere is formed (Figures 6a and 6b). As the inner angular velocity decreases with time, its effect on the secondary flow diminishes. During this time, the clockwise vortex grows considerably and after some time there is only one big counterclockwise vortex, which indicates that the outer sphere is dominating the flow. As seen in Figures 6c and 6d, the flow pattern tends towards a situation where the inner sphere is stationary, as one expects. Contours of ω for different time values are shown in Figure 7. Since the Reynolds number is large, these contours get closer to the inner sphere at the equator. In fact, for large Reynolds numbers (approximately larger than Re = 300), this secondary flow causes a considerable change in peripheral velocity (primary flow velocity profile). In general, the fluid particles in the vicinity of the equator move towards the inner sphere and return back towards the axis of rotation. As a result, a secondary distribution of peripheral velocity forms which affects the flow in the meridian plane again. As time advances, and if the Reynolds number is large, in the corner region between the outer sphere and equator line, the angular velocity contours move inwards and those contours in the vicinity of the axis of rotation move outwards. This effect can be described by considering the distribution of angular momentum. The rotation of the outer sphere provides a certain amount of angular momentum for the system that by the flow in the meridian plane and also Coriolis forces and nonlinear advection is redistributed. The fact that the total angular momentum of the azimuthal flow must be conserved by upward and downward moving fluid shows that the rotation of the upward moving elements of the fluid (near pole) slows down and the rotation of the downward moving elements of the fluid (near equator) speeds up.

The contours of T and $(T - T_c)$ for the inner angular velocity of $\Omega_{io} = -\exp(1-\tau)$, Re = 1000, Pr = 10, and Ek = 0 are shown in Figures 8 and 9. At

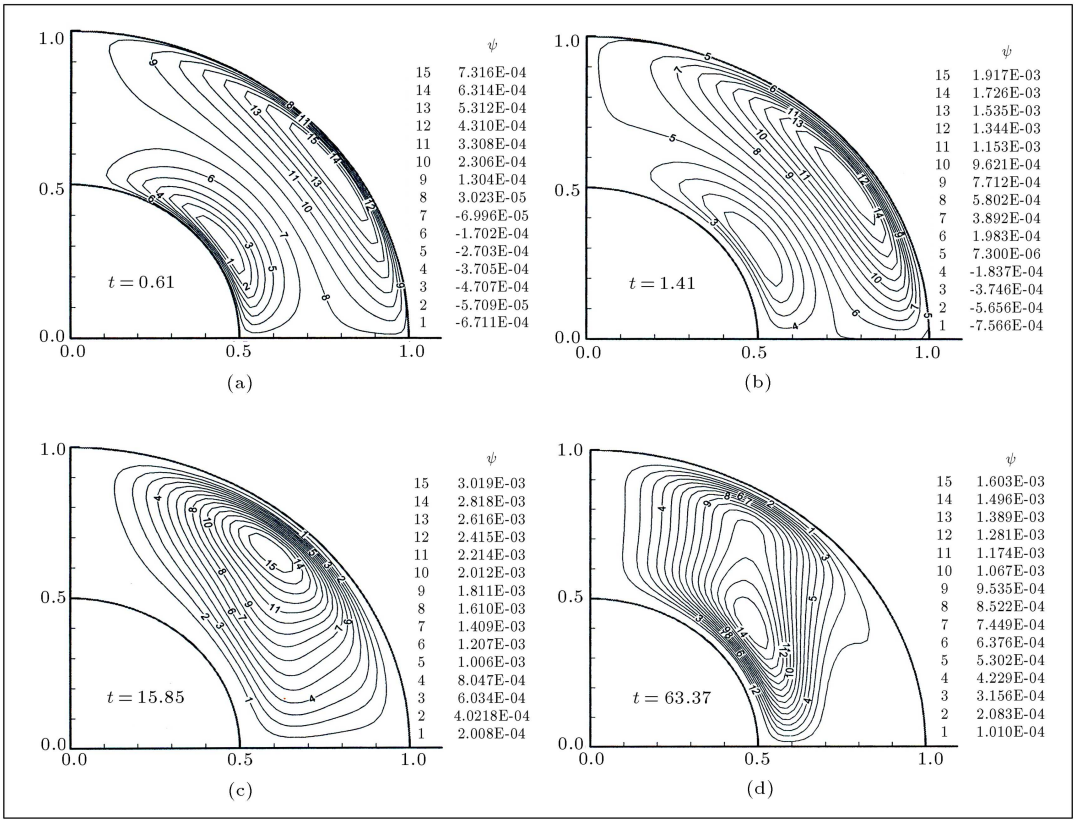

Figure 6. Contours of ψ for $\mathrm{Re} = 1000$ and $\Omega_{io} = -\exp(1-t)$.

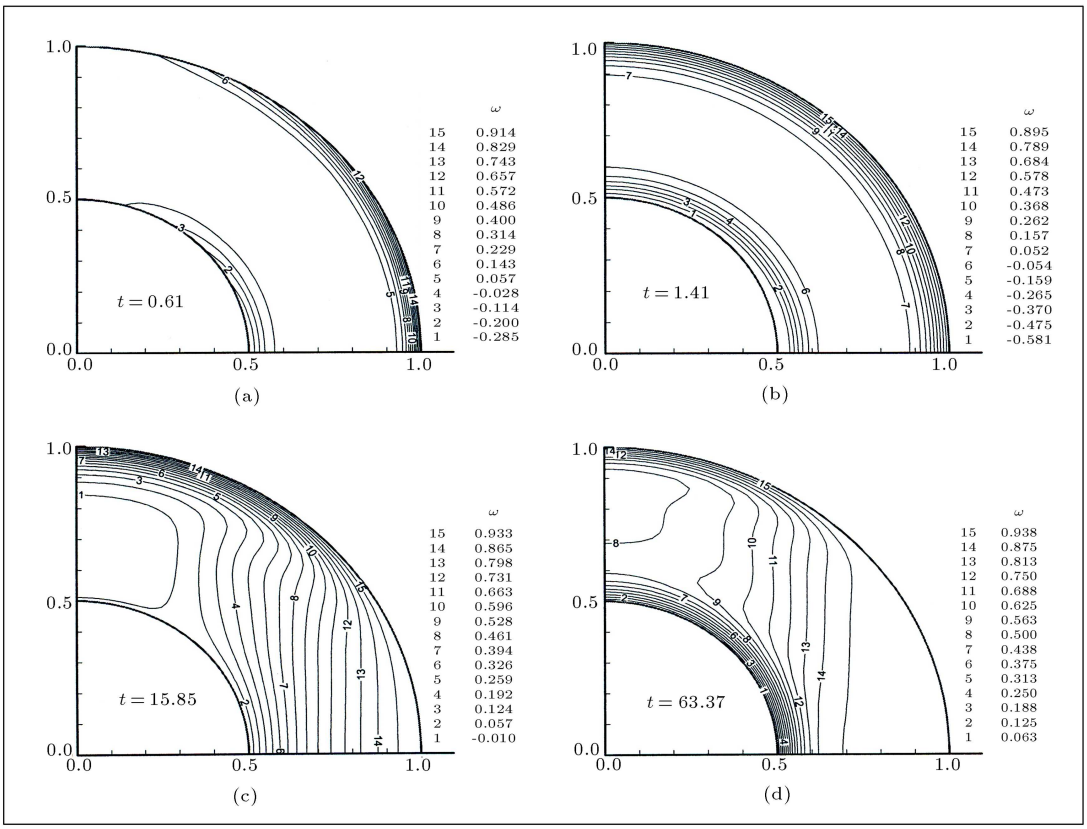

Figure 7. Contours of ω for $\mathrm{Re} = 1000$ and $\Omega_{io} = -\exp(1-t)$.

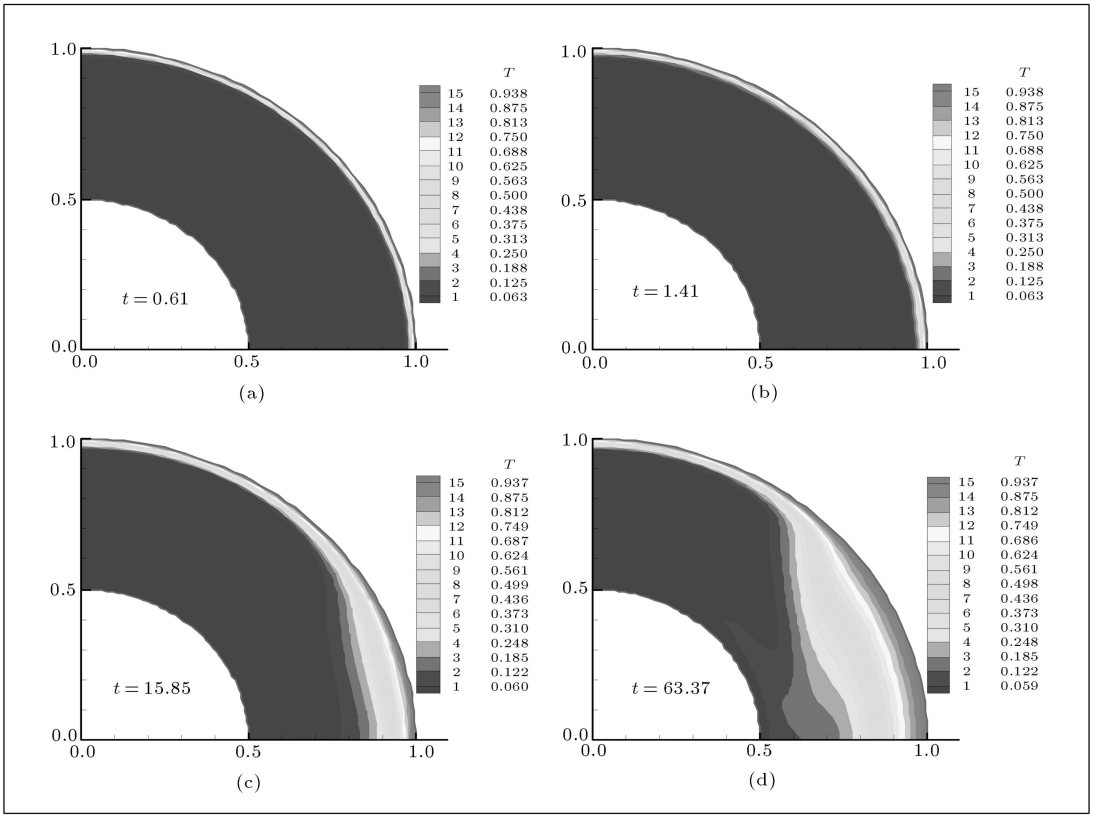

Figure 8. Contours of T for Re = 1000, Pr = 10, Ek = 0 and $\Omega_{io} = -\exp(1-t)$.

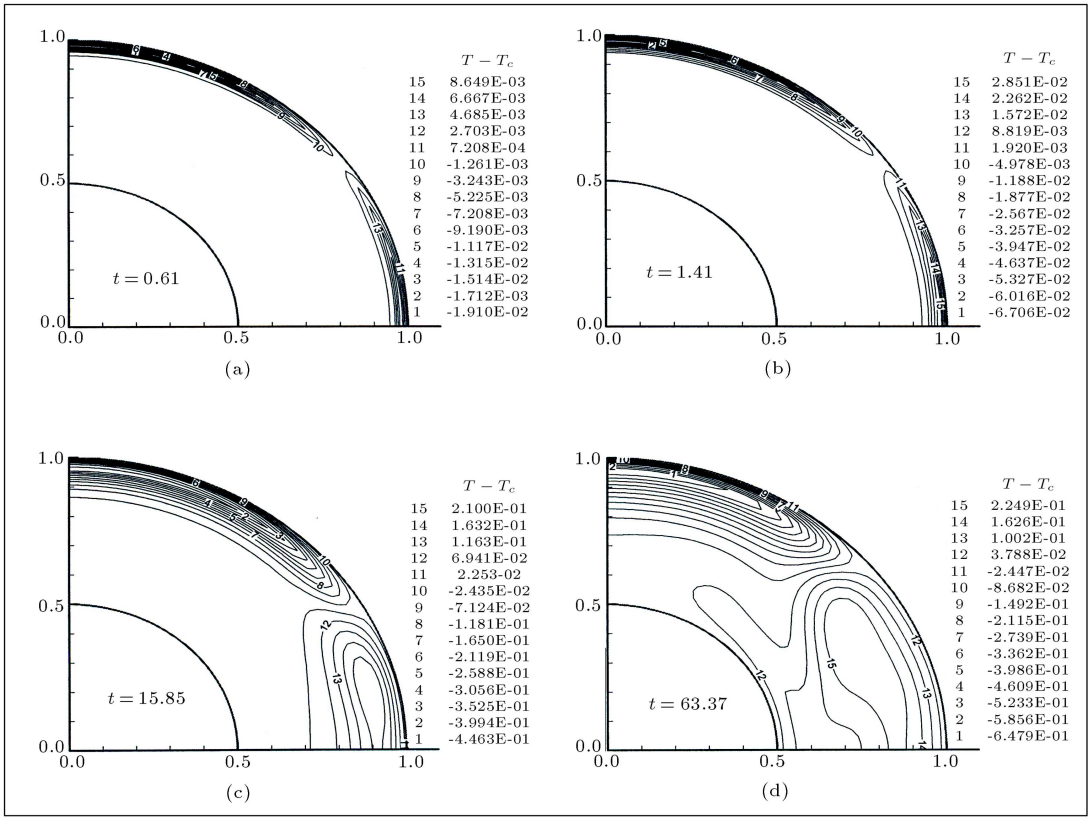

Figure 9. Contours of $(T - T_c)$ for Re = 1000, Pr = 10, Ek = 0 and $\Omega_{io} = -\exp(1-t)$.

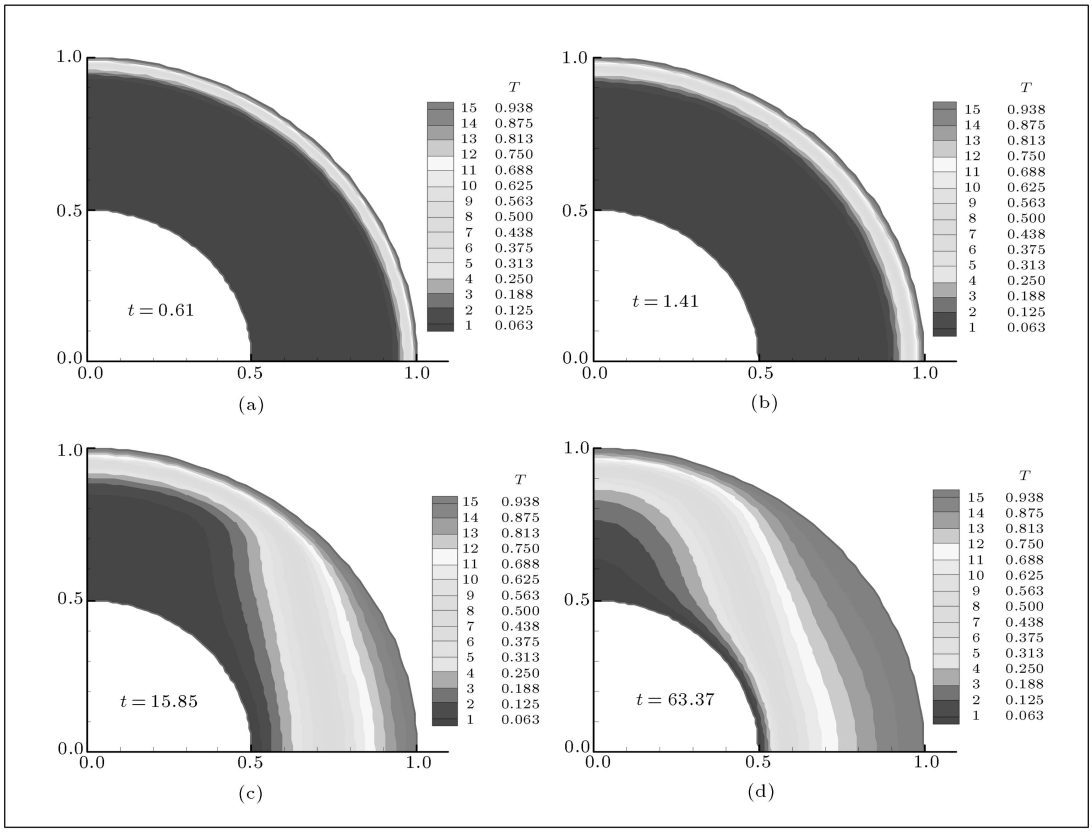

Figure 10. Contours of T for Re = 1000, Pr = 1, Ek = 0 and $\Omega_{io} = -\exp(1-t)$.

the outset, when both spheres dominate the flow, the diffusion of heat from the outer sphere into the field takes place approximately in a steady manner, but as the rotation effect of the inner sphere becomes weak, the temperature field grows considerably from the vicinity of the equator and affects the whole field. As far as $(T-T_c)$ contours, it is seen that at the beginning when the flow is forming, the difference between the actual temperature and the pure conduction temperature can be seen only in the region near the outer sphere, but as time passes, this difference becomes larger because of convection. It is obvious that this difference demonstrates itself in the form of positive and negative numbers. The contours near the pole are negative and those near the equator are positive. This is because the clockwise flow, which is formed by the rotation of the outer sphere, would transfer the heat of this sphere into the field and towards the equator and the inner sphere. On the contrary, as it moves along the inner sphere and rotation axis, it transfers the inner sphere coldness towards the outer sphere and the pole. As a result, in the vicinity of the pole, there are temperatures which are lower than pure conduction cases and in the vicinity of the equator there are temperatures which are higher than pure conduction cases. As evidenced in Figure 8, it is interesting to note that the angular velocities of spheres can cause long delays in the heat transfer of the fluid in large areas of the annulus around the poles.

Figures 10 and 11 present the T and $(T - T_c)$ contours for the same conditions as in Figures 8 and 9, except for Pr = 1. As seen in this case, the heat diffuses faster, because the heat diffusion mechanism by conduction is stronger than the diffusion of heat by convection, and also as the inner sphere rotates, a counterclockwise vortex is formed which curbs the heat convection and its transfer to the field. Therefore, when the Prandtl number is lower, the temperature field grows faster. This can be seen in Figure 11 where the contours are steadier. The difference between Figures 12 and 13, compared to Figures 10 and 11, is in the Eckert number. The Eckert number is related to viscous dissipation, which is the gradient of velocity that shows its effect as a source of heat in energy equations. This source, in fact, expresses the conversion of kinetic energy to heat energy, which causes the temperature of the flow field to rise. This effect (gradients of velocity) is seen in Figure 12 in which the temperature field has more expansion compared to Figure 10. Considering Figures 12 and 13, this difference is much clearer. These velocity gradients are the reason for the difference between the actual temperature and the case of pure conduction and can be seen better at the vicinity of the inner sphere in

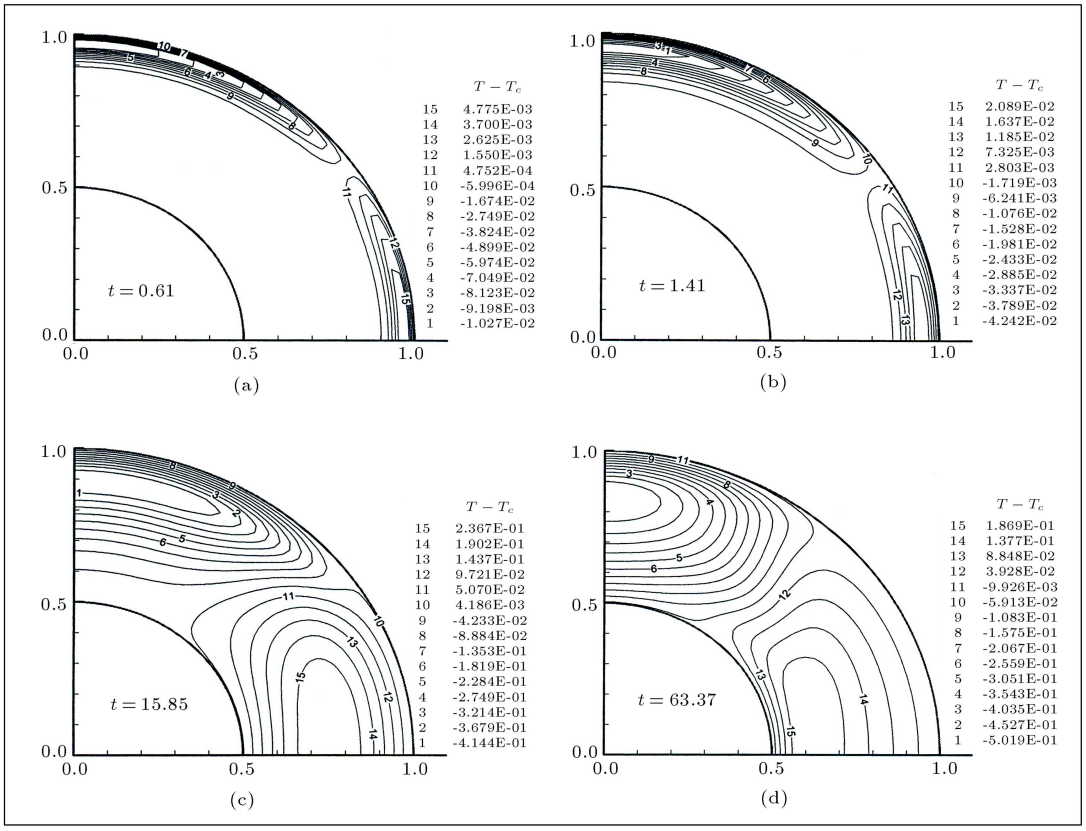

Figure 11. Contours of $(T - T_c)$ for Re = 1000, Pr = 1, Ek = 0 and $\Omega_{io} = -\exp(1 - t)$.

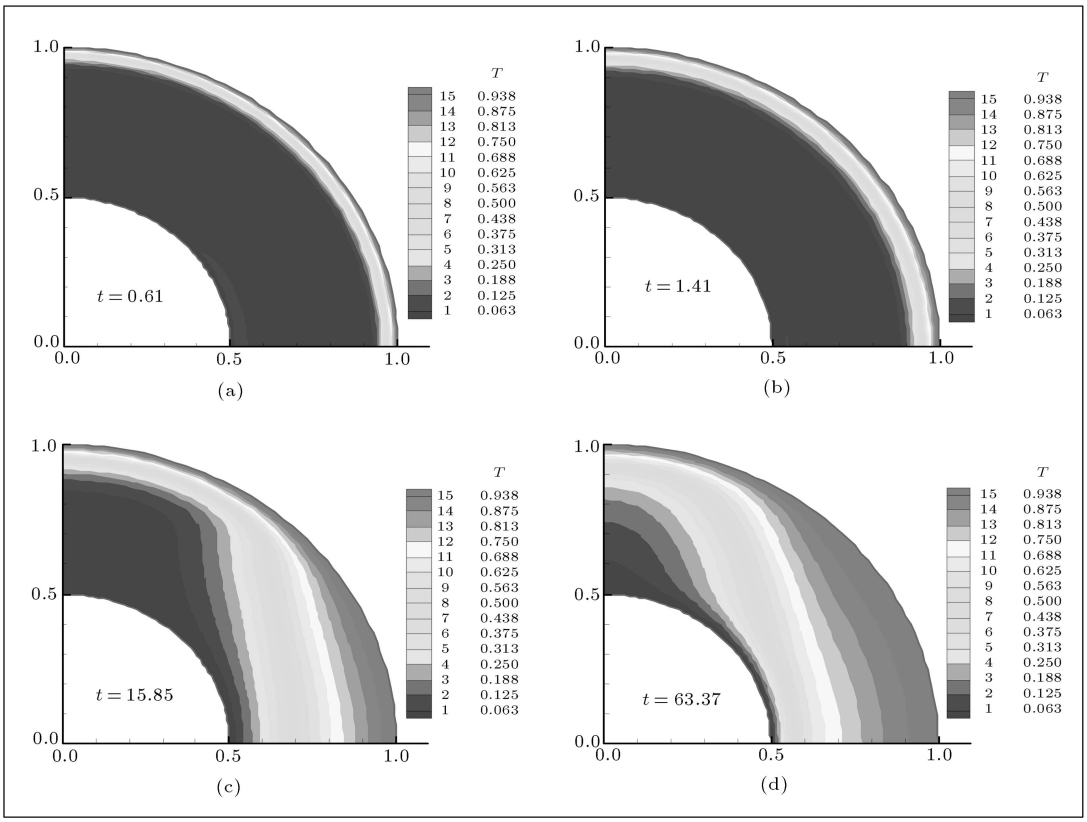

Figure 12. Contours of T for Re = 1000, Pr = 1, Ek = 0.001 and $\Omega_{io} = -\exp(1 - t)$.

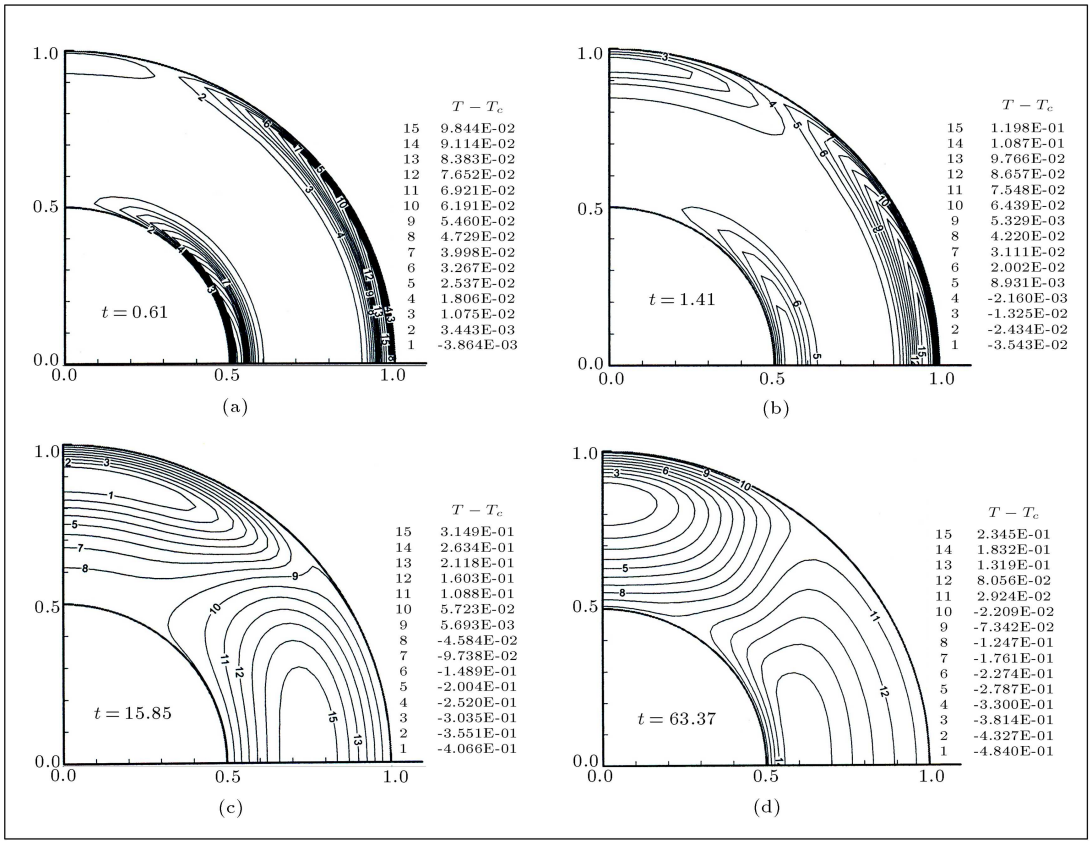

Figure 13. Contours of $(T - T_c)$ for Re = 1000, Pr = 1, Ek = 0.001 and $\Omega_{io} = -\exp(1-t)$.

Figures 12a and 12b, compared to Figures 10a and 10b. Also, as expected, the temperatures are higher when the dissipation terms are not omitted such as in [10].

Figures 14 to 17 have been drawn for inner angular velocity, $\Omega_{io} = 2\sin(\frac{\pi}{2}\tau)$, for Re = 1000, Pr = 10 and Ek = 0 and in two consecutive periods (second and third) for the sine function. As known, the sine function oscillates between -1 and 1. In these figures, the second and third periods after the sinusoidal movement have been considered. Inner sphere angular velocity in Figures 14a to 14d is approximately Ω_{io} = 0.0214, 1.998, -0.0214 and -1.998, respectively. The time values selected in these figures indicate the point at which the inner sphere velocity has come to an important change, showing that it has been considered immediately after a change of acceleration. For example, for the time value between case (a) and just before case (b), the inner sphere acceleration is positive and the time value at (b) is the starting point of negative acceleration for this sphere. As seen in Figure 15, the angular velocity of the fluid elements in the vicinity of the inner sphere is also dependent on past accelerations. This is because the inner sphere has a sinusoidal oscillation and, for example at τ = 4.01, when the inner sphere velocity is 0.0214 (a small positive value), it is seen that the fluid elements in its boundaries have a negative angular velocity, because in the one quart of the previous period, the inner sphere has a negative angular velocity. Therefore, as the outer sphere, containing a constant velocity, has a continuous and steady effect on the entire flow field, the inner sphere having an oscillating velocity between -2 and 2 (periodic acceleration of positive and negative) induces an unsteady and oscillatory type of effect on the layers in the vicinity of the inner sphere.

T and $(T - T_c)$ contours for the inner angular velocity of $\Omega_{io} = 2\sin(\frac{\pi}{2}\tau)$ are depicted in Figures 16 and 17 for Re = 1000, Pr = 10, and Ek = 0. Similar types of discussion, as in Figures 8 and 9, apply here as well. Also, the delay in heat transfer of the fluid in large portions of the annulus can be seen in Figure 16h.

CONCLUSIONS

A numerical study of the flow and heat transfer of a viscous incompressible fluid within a rotating spherical annulus has been investigated, when the spheres have time-dependent prescribed values of angular velocities. The characteristics of the flow and temperature fields are strongly dependent on the values of the various dimensionless parameters considered. The characteristics of angular velocity and temperature distribution

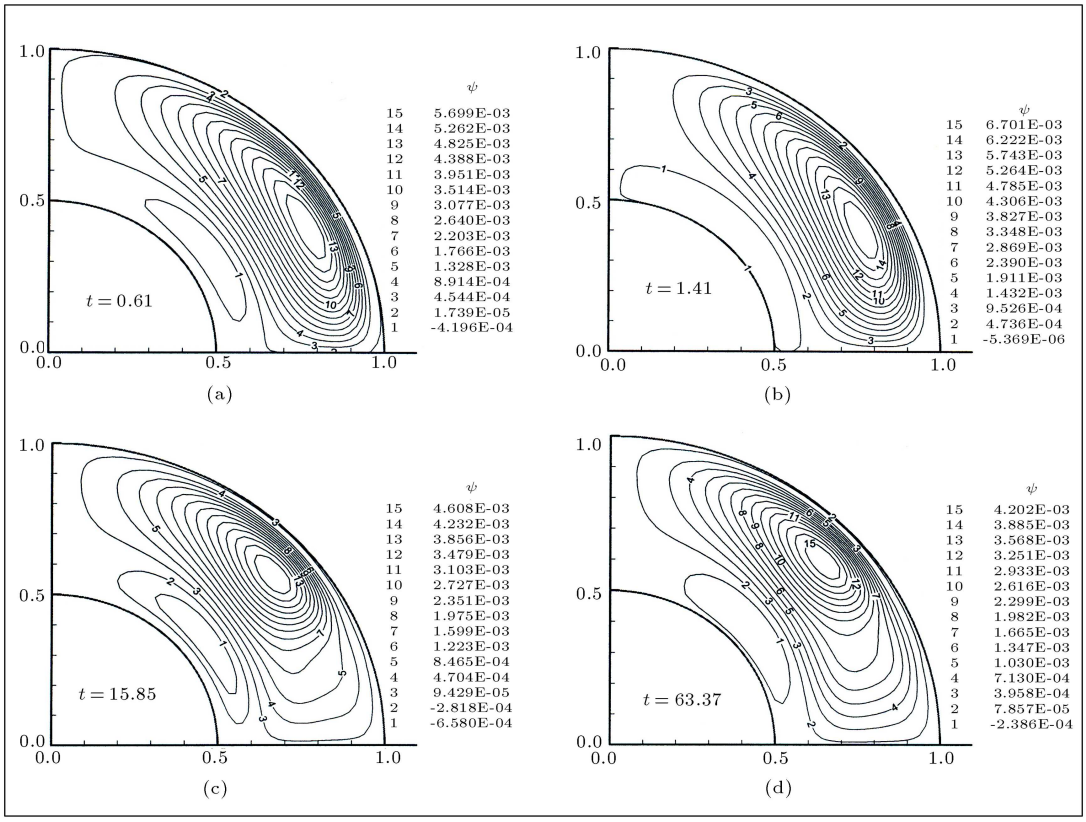

Figure 14. Contours of ψ for Re = 1000 and $\Omega_{io} = 2\sin(\pi/2)t$.

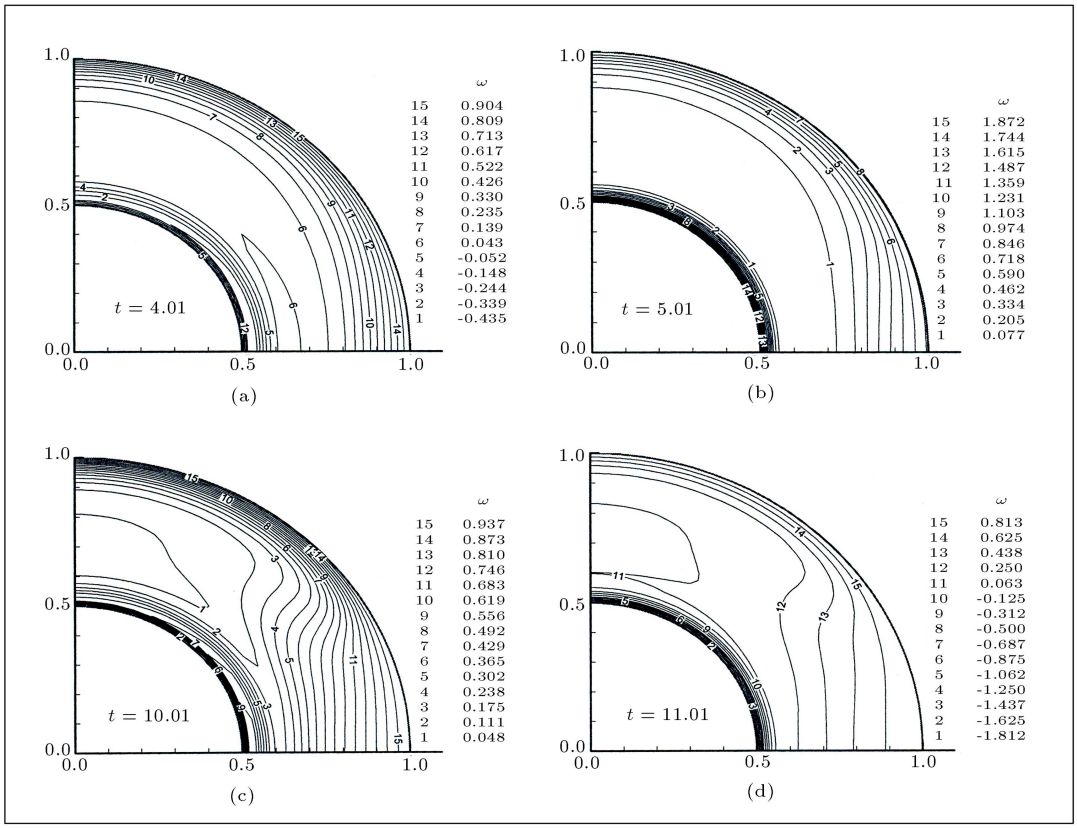

Figure 15. Contours of ω for Re = 1000 and $\Omega_{io} = 2\sin(\pi/2)t$.

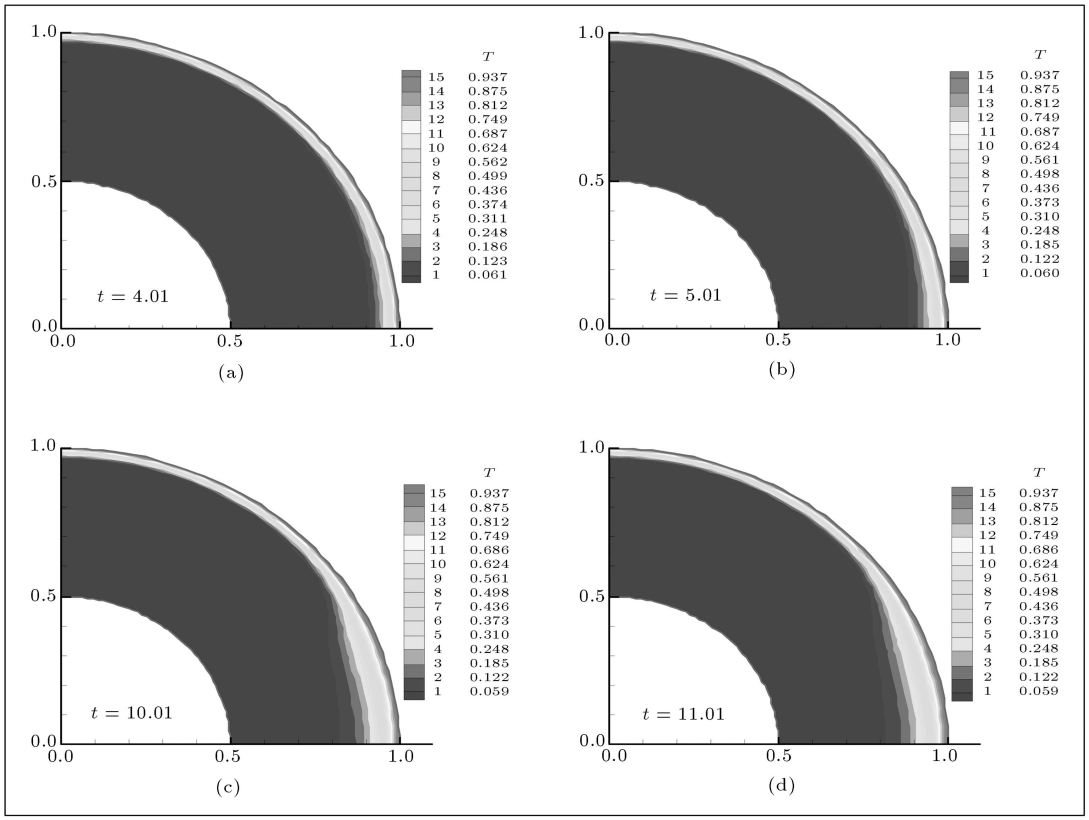

Figure 16. Contours of T for Re = 1000, Pr = 10, Ek = 0 and $\Omega_{io} = 2\sin(\pi/2)t$.

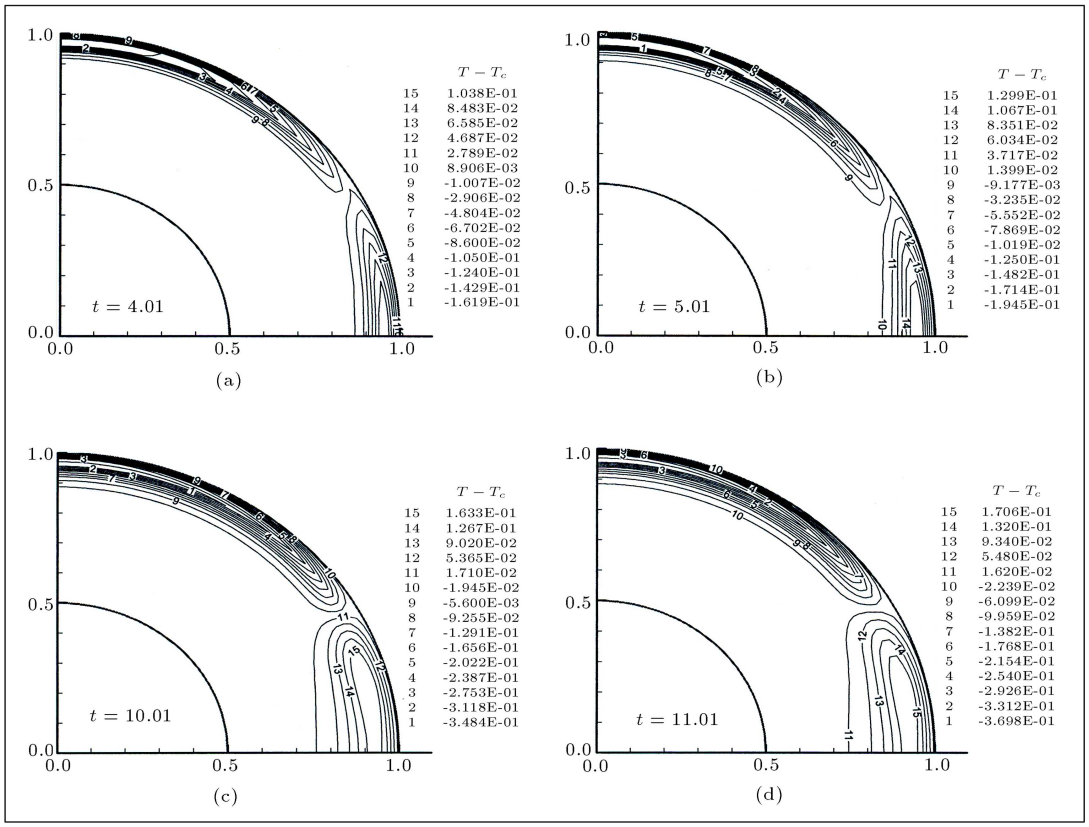

Figure 17. Contours of $(T - T_c)$ for Re = 1000, Pr = 10, Ek = 0 and $\Omega_{io} = 2\sin(\pi/2)t$.

for small Reynolds numbers are similar, which is expected, since, in this situation, there is a balance between the convection and diffusion of momentum and heat. At small Reynolds numbers, the secondary flow or vortices, which cause forced convection are weak, and hence the effect of convection and, therefore, the intensity of their local heat transfer do not exhibit a considerable difference from the pure conduction. But, for large Reynolds numbers, some deviations are seen in the angular velocity and temperature distributions, which indicate the effect of secondary flow on the primary flow. Since we have considered the case with time-dependent angular velocities, the relative velocities of the spheres are functions of time. Applying these angular velocities, shear layers are formed in the vicinity of the spheres, which get thicker because of a viscous diffusion effect and, depending on flow conditions, one or two circulations are formed in the meridian plane. An interesting effect of long delays in the heat transfer of a large portion of the fluid in the annulus is observed because of the angular velocities of the corresponding spheres.

NOMENCLATURE

b	$= R_i/R_0$
c	coefficient
c_P	specific heat at constant pressure
d	coefficient
e	coefficient
Ek	Eckert number
f	coefficient
$F(\eta)$	function
$G(\eta)$	function
$H(\eta)$	function
Pe	Peclet number
Pr	Prandtl number
r, θ, ϕ	spherical coordinates
r_0	reference value
Re	Reynolds number
R_i	inner sphere radii
R_0	outer sphere radii
T	temperature
T_i	inner sphere temperature
T_0	outer sphere temperature
v_r, v_θ, v_ϕ	velocity components

Greeks

α	thermal diffusivity
γ	function
τ	non-dimensional time
λ	function
η	similarity parameter
ν	kinematic viscosity
ψ	stream function
ω	angular velocity
ω_0	reference value
Ω	angular momentum function
Ω_i	inner sphere angular velocity
Ω_0	outer sphere angular velocity
Ω_{i0}	$= \Omega_i/\Omega_0$

REFERENCES

1. Howarth, L. "Note on boundary layer on a rotating sphere", *Philosophy Magazine Series*, **7**(42), pp. 1308-1311 (1951).
2. Proudman, I. "The almost rigid rotation of viscous fluid between concentric spheres", *Journal of Fluid Mechanics*, **1**, pp. 505-516 (1956).
3. Lord, R.G. and Bowden, F.P. " Boundary layer on a rotating sphere", *Proceeding of Royal Society A 271*, pp. 143-146 (1963).
4. Fox, J. "Singular perturbation of viscous fluid between spheres", *NASA TN D-2491*, pp. 1-50 (1964).
5. Greenspan, H.P. "Axially symmetric motion of a rotating fluid in a spherical annulus", *Journal of Fluid Mechanics*, **21**, pp. 673-677 (1964).
6. Carrier, G.F. "Some effects of stratification and geometry in rotating fluids", *Journal of Fluid Mechanics*, **24**, pp. 641-654 (1966).
7. Stewartson, K. "On almost rigid rotation", *Journal of Fluid Mechanics*, **26**, Part 1, pp. 131-144 (1966).
8. Pearson, C. "A numerical study of the time-dependent viscous flow between two rotating spheres", *Journal of Fluid Mechanics*, **28**, Part 2, pp. 323-336 (1967).
9. Munson, B.R. and Joseph, D.D. "Viscous incompressible flow between concentric rotating spheres, Part I: Basic flow", *Journal of Fluid Mechanics*, **49**, pp. 289-303 (1971).
10. Douglass, R.W., Munson, B.R. and Shaughnessy, E.J. "Thermal convection in rotating spherical annuli-1. Forced convection", *Int. J. Heat and Mass Transfer*, **21**, pp. 1543-1553 (1978).
11. Munson, B.R. and Douglass, R.W. "Viscous flow in oscillatory spherical annuli", *Journal of Physics of Fluids*, **22**(2), pp. 205-208 (Feb. 1979).
12. Gagliardi, J.C., Nigro, N.J., Elkouh, A.F. and Yang, J.K. "Study of the axially symmetric motion of an incompressible viscous fluid between two concentric rotating spheres", *Journal of Engineering Mathematics*, **24**, pp. 1-23 (1990).
13. Jen-Kang Yang, Nigro, N.J. and Elkouh, A.F. "Numerical study of the axially symmetric motion of an incompressible viscous fluid in an annulus between two

concentric rotating spheres", *International Journal for Numerical Methods in Fluids*, **9**, pp. 689-712 (1989).

14. Ni, W. and Nigro, N.J. "Finite element analysis of the axially symmetric motion of an incompressible viscous fluid in a spherical annulus", *International Journal for Numerical Methods in Fluids*, **19**, pp. 207-236 (1994).
15. Bar-Yoseph, P., Even-Sturlesi, G., Arkadyev, A., Solan, A. and Roesner, K.G. "Mixed convection of rotating fluids in spherical annuli", Lecture Notes in Physics 414, pp. 381-385 (1993).
16. Arkadyev, A., Bar-Yoseph, P. and Solan, A. "Thermal effects on axisymmetric vortex breakdown in a spherical gap", *Phys. Fluids A*, **5**(5), pp. 1211-1223 (1993).
17. Bar-Yoseph, P.Z. and Kryzhanovski, Y. "Axisymmetric vortex breakdown for generalized Newtonian fluid contained between rotating spheres", *Journal of Non-Newtonian Fluid Mechanics*, **66**(2-3), pp. 145-168 (1996).
18. Fendell, F.E. "Laminar natural convection about an isothermally heated sphere at small Grashof number", *J. of Fluid Mechanics*, **34**, pp. 163-176 (1968).
19. Caltagirone, J.P. "Natural convection between two concentric spheres-transition towards a multicellular flow", *Numerical Methods in Thermal Problems*, Pineridge Press, pp. 253-258 (1979).
20. Mack, L.R. and Hardee, H.C. "Natural convection between concentric spheres at low Rayleigh numbers", *Int. J. of Heat and Mass Transfer*, **11**, pp. 387-396 (1968).
21. Garg, V.K. "Natural convection between concentric spheres", *Int. J. of Heat and Mass Transfer*, **35**, pp. 1935-1945 (1992).
22. Chu, H.S. and Lee, T.S. "Transient natural convection heat transfer between concentric spheres", *Int. J. of Heat and Mass Transfer*, **36**(13), pp. 3159-3170 (1993).
23. Chiu, C.P. and Chen, W.R. "Transient natural convection heat transfer between concentric and vertically eccentric spheres", *Int. J. of Heat and Mass Transfer*, **39**(7), pp. 1439-1452 (1996).
24. Wu, H.W., Tsai, W.C. and Chou, H.M. "Transient natural convection heat transfer of fluids with variable viscosity between concentric and vertically eccentric spheres", *Int. J. of Heat and Mass Transfer*, **47**, pp. 1685-1700 (2004).
25. Press, W.H., Flannery, B.P., Teukolsky, S.A. and Vetterling, W.T. "Numerical recipes", *The Art of Scientific Computing*, Cambridge University Press, Cambridge (1997).